J Fluoresc (2011) 21:1155–1164
DOI 10.1007/s10895-010-0793-z

ORIGINAL PAPER

# Synthesis, Characterization Luminiscence Studies and Microbial Activity of Ethylenediamine Ruthenium (II) Complexes with Dipyridophenazine Ligands

**Mynam Shilpa · Penumaka Nagababu · Y. Praveen Kumar · J. Naveena Lavanya Latha · M. Rajender Reddy · K. S. Karthikeyan · Nazar Md. Gabra · Sirasani Satyanarayana**

Received: 4 October 2010 / Accepted: 9 December 2010 / Published online: 22 December 2010


**Abstract** Three symmetric ligands 7-methyl dipyrido-[3,2-a;2′,3′-c]phenazine (dppz-$CH_3$), 7-nitro dipyrido-[3,2-a;2′,3′-c]phenazine (dppz-$NO_2$) and benzo[i]dipyrido-[3,2-a;2′,3′-c]phenazine (dppn) and their ruthenium(II) complexes $[Ru(en)_2(L)][ClO_4]_2$ (en= ethylenediamine), L= dppz-$CH_3$, dppz-$NO_2$ and dppn have been synthesized and characterized by IR, $^1H$, $^{13}C$ NMR and Mass spectra. The interactions of these complexes with calf thymus DNA have been investigated by spectrophotometric, spectrofluorimetric, circular dichroism, viscosity and thermal denaturation studies. As the planar extension of the intercalative ligand increases, the interaction of the complex with DNA increases, indicating that the size and shape of the intercalalative ligand has a marked effect on the strength of interaction. The plot of log K versus log $[Na^+]$ yield a slope of -1.26, -1.53, -1.60 for the complexes 1, 2 and 3 respectively. These three complexes have been found to promote the cleavage of plasmid pBR 322 DNA upon irradiation.

**Keywords** Symmetric ligands · Transition metal · Fluorescence studies · Salt dependence studies · Toxicity studies

M. Shilpa · P. Nagababu · Y. P. Kumar · M. R. Reddy · N. M. Gabra · S. Satyanarayana (✉)
Department of Chemistry, Osmania University, Hyderabad, Andhra Pradesh, India PIN-500007
e-mail: ssnsirasani@gmail.com

J. N. L. Latha
Krishna University, Machilipatnam, India

K. S. Karthikeyan
National Institute of Nutrition, Hyderbad, India

## Introduction

1,10-phenanthroline has a rigid framework and possesses a superb ability to chelate many metal ions via two nitrogen donors, which show potential for technological applications, due to their high charge transfer mobility, bright light-emission and good electro- and photo-active properties [1–5]. Varying substitutive group or substituent position in the intercalative ligand can create some interesting differences in the space configuration and the electron density distribution of Ru(II) polypyridyl complexes, which result in some differences in spectral properties and the DNA-binding behaviors of the complexes, and are helpful to understand the binding mechanism of Ru(II) polypyridyl complexes to DNA. Therefore, further studies using different structural ligands to evaluate and understand the factors that determine the DNA-binding mode are necessary. Thus it is of interest to delineate the effects of the planarity of the intercalative ligand on interaction and the binding mode of the complexes to DNA. Barton and co-workers have pioneered the application of polypyridyl transition metal complexes as tools to probe recognition of double helical DNA using coordination complexes, matching their shapes, symmetries, and functionalities to sites along the strand [6–11]. Earlier they reported the DNA-binding behaviors of bipyridine, phen, ip, pip, pyip and aip of ethylenediamine Ru(II) complexes [12, 13]. Metallointercalators that contain an extended aromatic heterocyclic ligand can provide immensely powerful tools to probe nucleic acids [14–20].

In fact, molecular shape which contributes to stabilizing the metal complex on the DNA helix is one of the most significant factors [21]. Herein we report the synthesis of dppz substituted ligands L = dppz-CH3 (**a**), dppz-NO2 (**b**)

and dppn (**c**) and their complexes with ruthenium(II) ethylenediamine $[Ru(en)_2(dppz\text{-}CH_3)]$ (**1**) $[Ru(en)_2(dppz\text{-}69\ NO_2)]$ (**2**) and $[Ru(en)_2(dppn)]$ (**3**) and their DNA-binding properties have been studied. This includes photocleavage studies as well as the toxicity of these complexes to yeast.

## Experimental

### Physical Measurements

IR spectra were recorded, in KBr phase on Perkin-Elmer FTIR-1605. $^1H$ , $^{13}C$-NMR spectra were recorded on a *Varian XL-300 & 200 MHz* spectrometer with DMSO-$d_6$ + $CDCl_3$ as a solvent at room temperature and tetramethylsilane (TMS) as the internal standard. $Es^+$-MS mass spectra were recorded on *JEOL SX 102/DA-6000 mass spectrometer/data system*. UV-Visible spectra were recorded on an *Elico Bio-spectrophotometer model BL198*. Emission measurements were carried out by using a *Elico Bio-spectrofluorimeter model SL174*. Circular dichroism spectra were recorded on *JASCO J-810 spectropolarimeter*. Viscosity experiments were carried out in an *Ostwald viscometer* maintained at a constant temperature 30.0±0.1 °C in a thermostatic water-bath.

### Materials and Methods

The compounds 1, 10, phenanthroline-5, 6-dione [22] were synthesized according to literature procedure. All chemicals were of reagent grade. A solution of calf thymus DNA in buffer gave a ratio of 1.8–1.9 UV absorbance at 260 and 280 nm indicating that DNA was sufficiently free of protein [23]. The DNA concentration per nucleotide was determined by using a molar absorption coefficient (6600 $M^{-1}$ $cm^{-1}$) at 260 nm [24].

### Synthesis of Ligands

(dppz-$CH_3$) 7-methyl dipyrido-[3,2-a;2′,3′-c] phenazine.

The ligand was synthesized according to the procedure in the literature [25]. A mixture of phen-dione (0.210 g, 1 mmol), 4-methyl benzene1,2diamine (0.122 g, 1 mmol) was refluxed together in ethanol (20 ml) for 4-hrs. The solution was cooled to room temperature, to get light-yellow precipitate of dppz-$CH_3$, which was suctioned and the compound filtered. It was recrystalized from cold ethanol. (yield: 70%). Analytical data: $Es^+$-MS Cal:296, Found: 297. $^1H$-NMR (300 MHz, ppm DMSO-$d_6$, TMS) 9.65(d, 2H), 8.50(d, 2H), 8.32(d, 2H), 8.03(s, 1H), 7.85(d, 1H), 7.02(d, 1H), 2.34(s, 3H). $^{13}C$ [$^1H$] NMR (200 MHz , ppm, DMSO-$d_6$, major peaks): 151.6,143.20, 136.5, 133.5, 132.0, 129.0, 127.7, 126.0, 120.0, 22.30.

(dppz-$NO_2$) 7-nitro dipyrido-[3,2-a;2′,3′-c] phenazine.

The ligand was synthesized according to the above procedure by refluxing Phen-dione (0.210 g, 1 mmol) and 4-nitrobenzene1,2diamine (0.158 g, 1 mmol). Finally orange-yellow precipitate obtained. Recrystalized from aq. methanol. (yield: 68%). Analytical data: $Es^+$-MS Cal: 327, Found: 328. $^1H$-NMR (300 MHz, ppm DMSO-$d_6$, TMS) 9.85(d, 2H), 9.30(m, 2H), 8.95(m, 1H), 8.70(m, 1H), 8.50 (m, 1H), 7.80(d, 2H). $^{13}C$ [$^1H$] NMR (200 MHz , ppm, DMSO-$d_6$, major peaks): 151.8, 141.2, 134.5, 132.2, 131.0, 128.5, 126.7, 124.3, 118.

(dppn) benzo[i] dipyrido-[3,2-a;2′,3′-c] phenazine.

The ligand was synthesized according to the above procedure refluxing the mixture of phen-dione (0.210 g, 1 mmol) and 1,2diaminonaphthalene (0.176 g, 1 mmol), pale yellow precipitate was formed. Recrystalized from aq. methanol. (yield: 68%). Analytical data: $Es^+$-MS Cal: 332, Found: 333. $^1H$-NMR (300 MHz, ppm DMSO-$d_6$, TMS) 9.25(d, 2H), 9.22(m, 2H), 8.19(d, 2H), 7.83(dd, 2H), 7.65 (d, 2H). $^{13}C$ [$^1H$] NMR (200 MHz, ppm, DMSO-$d_6$, major peaks): 150.9, 144.5, 141.13, 140, 139.6, 138.1, 135, 134, 128.1, 127, 126.7, 125, 124.2, 123.8.

### Synthesis of Complexes

$$\left[Ru(en)_2(dppz-CH_3)\right](ClO_4)_2$$

Cis $[Ru(en)_2Cl_2]Cl$ complex was prepared according to the literature method [26]. A mixture of Cis $[Ru(en)_2Cl_2]Cl$ (0.074 g, 0.25 mmol) and dppz-$CH_3$ ( 0.030 g, 0.25 mmol) were placed in a 100 ml round-bottom flask containing 20 ml of methanol and refluxed for 5-hours. The resulting brownish-red solution was allowed to cool at room temperature and then $NaClO_4$ in methanol was added. The thick crystalline precipitate of $[Ru(en)_2dppz\text{-}CH_3]^{2+}$ that formed was collected and recrystalized from acetone/water, (yield: 61%). Analytical data: $Es^+$-Ms: Cal: 716, Found: 715. IR: 1404 (C=C), 1615 (C=N), 739 (Ru–N (L)) & 668 $cm^{-1}$ (Ru–N (en)). $^1H$-NMR (300 MHz, ppm DMSO-$d_6$, TMS) δ: 9.7 (d, 2H), 9.4 (s, 1H), 8.2 (d, 2H), 7.9 (d, 1H) , 7.8 (d, 1H), 7.7 (t, 2H), 1.2 (methyl peak, s, 3H), 2.8 & 3.1 (en peaks). $^{13}C$ [$^1H$] NMR (200 MHz, ppm DMSO-$d_6$ , major peaks): 152.1, 147.1, 140.5, 139.3, 135.3, 132.9, 128.57, 127.41, 126.7, 124.5, 44.73 , 34.20 and 29.14 (methyl peak).

$$\left[Ru(en)_2(dppz-NO_2)\right](ClO_4)_2 2H_2O$$

The complex was synthesized by the above method. Cis $[Ru(en)_2Cl_2]Cl$ (0.074 g, 0.25 mmol) and dppz-$NO_2$ (0.035 g, 0.25 mmol) (yield: 55%). Analytical data: $Es^+$-Ms: Cal: 783, Found: 785. IR: 1418 (C=C), 1492 (C=N), 737 (Ru–N (L)) & 661 $cm^{-1}$ (Ru–N (en)). $^1H$-NMR (300 MHz, ppm DMSO-$d_6$, TMS) δ: 9.92 (d, 2H), 9.6 (s,

1H), 8.2 (d, 2H), 8.09 (d, 1H), 7.9(d, 1H) 7.8 (t, 2H), 2.6 & 3.1 (en peaks). $^{13}C$ [$^{1}H$] NMR (200 MHz, ppm DMSO-$d_6$ + $CDCl_3$, major peaks): 155.67, 154.07, 126.96, 125.32, 123.17, 43.27, 30.6.

$$\left[Ru(en)_2(dppn)\right](ClO_4)_2 0.5H_2O$$

The complex was synthesized by the above method. Cis $[Ru(en)_2Cl_2]Cl$ (0.074 g, 0.25 mmol) and dppn (0.039 g, 0.25 mmol). (yield: 59%). Analytical data: $Es^{+}$-Ms: Cal: 758, Found: 759. IR: 1420 (C=C), 1440(C=N), 720 (Ru–N (L)) & 669 $cm^{-1}$ Ru–N (en) $^{1}H$-NMR (300 MHz, ppm DMSO-$d_6$, TMS) δ: 9.6 (d, 2H), 9.2 (d, 2H), 9.1 (d, 2H), 8.2 (d, 2H), 8.1 (m, 4H) , 2.8 & 3.1 (en peaks). Structure of the complexes are shown in Fig. 1.

## DNA Binding Studies

Interaction of the ruthenium complexes with DNA was studied in tris-buffer. In the emission studies fixed metal complex concentration (6 μM) was taken and varying concentration (0–150 μM) of DNA was added. The excitation wavelength was fixed and the emission range was adjusted before measurements. The fraction of the ligand bound was calculated from the relation $C_b = C_t[(F - F_0)/F_{max} - F_0)]$, where $C_t$ is the total complex concentration, F is the observed fluorescence emission intensity at a given DNA concentration, $F_0$ is the intensity in the absence of DNA, and $F_{max}$ is when the complex is fully bound to DNA. Binding constant of fluorescence was obtained from a modified Scatchard equation [27] A plot of $r/c_f$ vs r, where r is the $C_b$/[DNA] and $c_f$ is the concentration of the free complex.

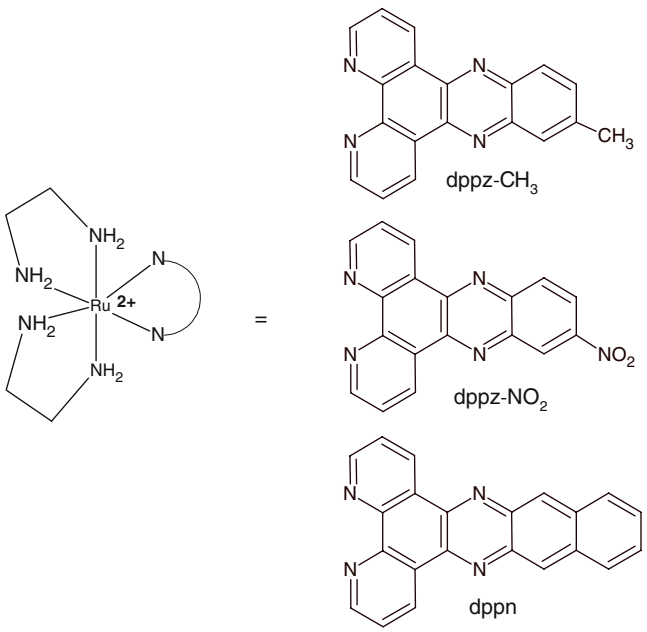


**Fig. 1** Structure of the complexes

Fluorescence quenching experiment was carried out by the addition of 0.1 M of $[Fe(CN)_6]^{4-}$ and 1.5 M of KI as quencher, to the complex alone and in presence of DNA. According to the classical Stern-Volmer equation [28]

$$I_0/I = 1 + K_{sv}[Q]$$

Where $I_0$ and I are the luminescence intensities in the absence and presence of quencher $[Fe(CN)_6]^{4-}$ or KI respectively. K is a linear Stern-Volmer quenching constant depending on the ratio of the bound concentration of the complex to the concentration of DNA. [Q] is the concentration of the quencher $[Fe(CN)_6]^{4-}$ or KI. In the plot of $I_0$/I versus [Q] the linear Stern-Volmer quenching constant $K_{sv}$ is given by the slope. The absorption titration of the metal complex in buffer were performed by titrating fixed concentration of complex (15 μM) to which the increments of DNA was added (0-130 μM). The intrinsic binding constant, $K_b$ was calculated from below equation [29]

$$[DNA]/(\varepsilon_a - \varepsilon_f) = [DNA]/(\varepsilon_b - \varepsilon_f) + 1/(K_b(\varepsilon_b - \varepsilon_f))$$

Where [DNA] is the concentration of DNA. $\varepsilon_a$ $\varepsilon_f$ and $\varepsilon_b$ corresponds to the extinction coefficient for the free metal complex, the complex in the presence of DNA and complex in the fully bound form respectively. In the plots of [DNA]/($\varepsilon_a$–$\varepsilon_f$) versus [DNA], $K_b$ is given by the ratio of slope to intercept.

Viscosity experiments were carried out in an Ostwald viscometer maintaining at a constant temperature 30.0±0.1 °C in a thermostated water-bath. Calf thymus DNA samples approximately 200 base pairs were prepared by sonicating in order to minimize complexities arising from DNA flexibility [30]. Flow time was measured with a digital stop watch and each sample was measured three times, and then an average flow time was calculated. Data were presented as $(\eta/\eta_0)^{1/3}$ vs. the complex /[DNA]. Where η is the viscosity of DNA in presence of complex and $\eta_0$ is the viscosity of DNA alone. Viscosity values were calculated from the observed flow time of DNA and DNA + complex [31].

Thermal denaturation studies were carried out with a *spectrophotometer*, by monitoring the absorbance at 260 nm taking the complex as (20 μM) and DNA as (120 μM) [32]. Salt dependence studies were performed in tris buffer by titrating preformed complex-DNA adduct with NaCl solution.

Photocleavage studies were carried out in a total volume of (10 μl) containing pBR322 DNA (0.1 μg) and different complexes with varying concentration were incubated for

30 min in the dark and then irradiated at room temperature with a UV lamp 302 nm, for 1/2 h. Samples were analyzed by electrophoresis for 2.5 h at 40 V on a 0.8% agarose gel in buffer, $p^H$ 8.2. The gel was stained with 1μg/ml ethidium bromide and then photographed under UV light. Photocleavage studies using histidine was also carried to know the mechanism of cleavage.

Circular dichroism spectra of DNA were obtained by using *JASCO J-810 spectropolarimeter* operating at 25 °C with 3 $cm^3$ of Calf thymus DNA (90μM$dm^{-3}$) sealed in a dialysis bag and 6 $cm^3$ of the complex (30μM$dm^{-3}$) outside the bag and the system agitated on a shaker bath for 24 h. The region between 210 to350nm was scanned for each sample. Molecular ellipticity values were calculated according to the formula

$$[\theta]_\lambda = [\theta_\lambda / Cl] \times 100$$

Where $[\theta]_\lambda$ is the Molecular ellipticity value at a particular wavelength expressed in degrees centimeter squared per mole, C is the concentration of nucleotide phosphates per liter, l is the length of the cell in cm and $\theta_\lambda$ is observed rotation in degrees.

Toxicity studies were performed on yeast [Saccharomyces cerevisiae (NCIM3558)] as a test organism. Strains maintained on YEPD (Yeast Extract Peptone Dextrose) agar were inoculated in to 250 ml conical flask with 100 ml YEPD broth containing yeast extract-10 g/l, peptone-20 g/l, Dextrose-30 g/l, $KH_2PO_4$-0.5 g/l, $K_2HPO_4$-0.5 g/l, $MgSO_4.7H_2O$-0.5 g/l, $(NH_4)_2SO_4$-2 g/l , $P^H$ 5.0 and were incubated at 30 °C on a shaker at 250 rpm.

## Results and Discussion

### Steady-State Emission Studies

The interaction of the Ru(II) complexes with the double helix CT-DNA was monitored via luminescence. Upon the addition of CT-DNA, the emission of complex (3) exhibits pronounced enhancement. However, the emission intensities increase by 3.85 and 4.20 & 4.35 for complexes (1), (2) and (3), respectively as shown in Fig. 2. In the presence of DNA the complex interacts strongly with DNA and can be efficiently protected by DNA, since the hydrophobic environment inside the DNA helix reduces the accessibility of solvent water molecules to the complex and the complex mobility is restricted at the binding site, leading to decrease of the vibrational modes of relaxation [33, 34]. The binding constant for 1, 2 & 3 (Table 1) complexes was found to be slightly lower than that obtained by the absorption titration method. The different $K_b$ values obtained by the two titration

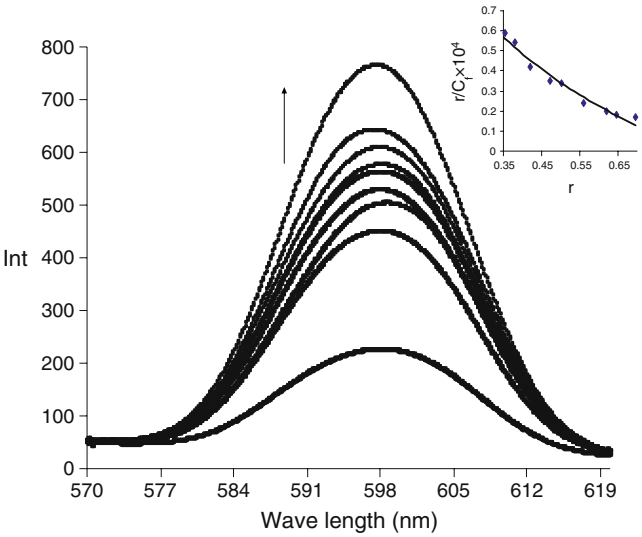


**Fig. 2** Fluorescence Emission spectra of complex (1) $[Ru(en)_2dppz\text{-}CH_3]$in tris buffer in the presence of CT DNA, [Ru]=10μL($3\times10^{-6}$), [DNA]=0–150 μM. $\lambda_{exc}$=459 nm, $\lambda_{emi}$=598 nm.The insert shows the best fit of data to $r/c_f$ versus r

methods of measurements (absorption and Fluroscence titration), as recently suggested by Wu et al. [35], these values are in complete agreement with that of absorption spectroscopy.

### Fluorescence Quenching

Steady-state emission quenching experiments using $[Fe(CN)_6]^{4-}$ and KI as quenchers may provide further information about the binding of complexes with DNA. In the absence of DNA the emission of complex was efficiently quenched by the quencher and the plots are not linear which imply that the quenching process is both static and dynamic [36]. This may be explained by repulsions of the highly negative $[Fe(CN)_6]^{4-}$ from the DNA poly anion backbone which hinders access of $[Fe(CN)_6]^{4-}$ to the DNA bound complexes [37]. The ferro-cyanide and KI quenching curves for 1, 2 & 3 complexes in the presence of CT DNA can be understood by the following classical Stern-Volmer equation [29], which also indicates that the complexes bind to DNA. However in the presence of DNA, the Stern-Volmer plots are changed drastically. This

**Table 1** Emission data of complexes

| Complexes | Ex peak | Em peak | Fluroscence Binding const |
|---|---|---|---|
| $[Ru(en)_2dppz\text{-}CH_3]^{2+}$ | 468 | 598 | $4.8\times10^4$ |
| $[Ru(en)_2dppz\text{-}No_2]^{2+}$ | 457 | 584 | $2.81\times10^5$ |
| $[Ru(en)_2dppn]^{2+}$ | 411 | 511 | $3.8\times10^5$ |

dppz-$CH_3$ , dppz-$NO_2$, dppn ligands ex =459,420,400; em = 510,502,480.

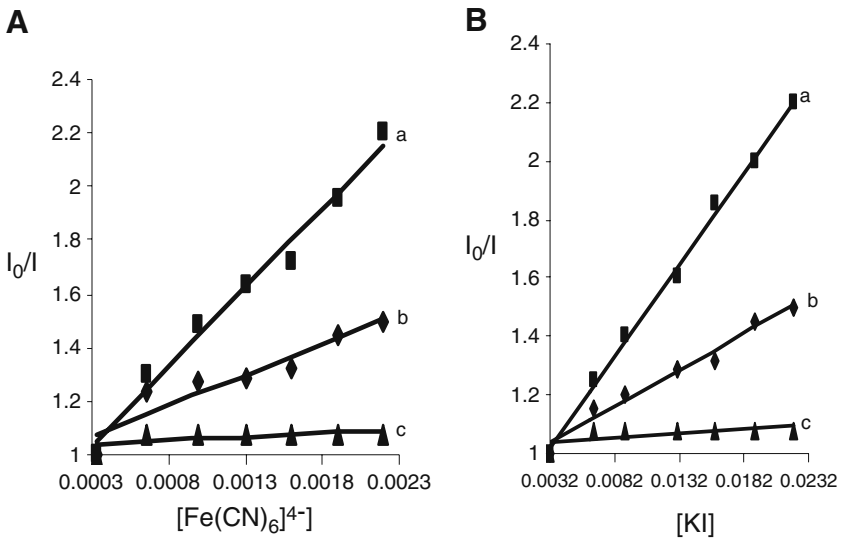


**Fig. 3** Emission quenching of complex $[Ru(en)_2dppn]^{2+}$ with $[Fe(CN)_6]^{4-}$ (**A**) and KI (**B**) in the absence of DNA (**a**), presence of DNA1:20 (**b**), 1:200(**c**) $[Ru]=(3\times10^{-6})$

may be explained by repulsions of the highly negative $[Fe(CN)_6]^{4-}$ from the DNA polyanion backbone which hinders access of $[Fe(CN)_6]^{4-}$ to the DNA bound complexes. A larger slope for the Stern-Volmer curve parallels poorer protection and low binding. Comparing this with ferrocyanide, KI shows less quenching affinity, because KI is mononegative, whereas ferrocyanide is tetra negatively charged. Due to this ferrocyanide quencher is four times more than KI. Ferrocyanide quenching & KI fluorescence quenching curves of complexes when bound to DNA are given in Fig. 3 and $K_{sv}$ values are given in (Table 2). From absorption and fluorescence spectroscopy studies the binding of complexes with DNA is in the order 3>2>1.

## Electronic Absorption Titration

Absorption spectroscopy is the most convenient tool for examining the interaction of complexes with DNA. As a general observation, the binding of intercalative molecules to DNA is accompanied by a red shift and hypochromism in the absorption spectra. The extent of hypochromism is commonly consistent with the strength of the intercalative interaction [9, 38, 39]. In the presence of increasing concentrations of calf thymus DNA, the intraligand ($\pi$-$\pi^*$) and metal-to-ligand (MLCT) $d_{Ru}\rightarrow\pi^*_{L\text{-}L}$ transitions of the complex were significantly perturbed, indicating interaction of the complex with DNA. The electronic absorption spectra of the polypyridyl ruthenium(II) with ethylenediamine in the absence and in presence of CT-DNA in tris-buffer are given in Fig. 4. Upon the addition of CT-DNA, the electronic absorptions of 1, 2 and 3 complexes experienced significant hypochromism, for complex (1) 7.6%, complex (2) 10.4% and complex (3) 12.1%. Since the main ligand intercalates into the base pairs of DNA, the $\pi^*$ orbital of the intercalating ligand can couple with $\pi$ orbital of the base pairs, the coupling $\pi^*$ orbital is partially filled by electrons, thus decrease the transition probabilities and concomitantly resulting in change in hypochromism [40]. These data preliminarly imply that these complexes bind to DNA in a intercalative mode [41]. In order to further investigate the binding strength of the complex, the intrinsic binding constants $K_b$ of the three complexes, were calculated by the equation [27] as $1.7\times10^4$ complex (1), $2.5\times10^5$ complex (2) & $3.6\times10^5$ complex (3). The binding constant of these complexes are smaller when compared to the similar complexes with different ancillary ligands like phen, bpy $[Ru(phen)_2(dppz\text{-}NO_2)]$ $(3.5\times10^5)$, $[Ru(bpy)_2(dppz\text{-}NO_2)$ $(2.92\times10^5)$, $[Ru(phen)_2(dppz\text{-}CH_3)]$ $(3.13\times10^5)$ and $Ru(bpy)_2(dppz\text{-}CH_3)]$ $(2.31\times10^5)$ [42].

**Table 2** $K_{sv}$ values of complexes

| Complexes | Complex | $Fe(CN)_6]^{4-}$ | | Complex | KI | |
|---|---|---|---|---|---|---|
| | | Complex+DNA | | | Complex+DNA | |
| | | 1:20 | 1:200 | | 1:20 | 1:200 |
| $[Ru(en)_2dppz\text{-}CH_3]^{2+}$ | 523.4 | 320.6 | 36.5 | 50.6 | 33.5 | 3.76 |
| $[Ru(en)_2dppz\text{-}No_2]^{2+}$ | 565.0 | 275.3 | 32.5 | 57.3 | 30.9 | 3.54 |
| $[Ru(en)_2dppn]^{2+}$ | 593.3 | 229.7 | 29.0 | 62.8 | 25.1 | 2.81 |

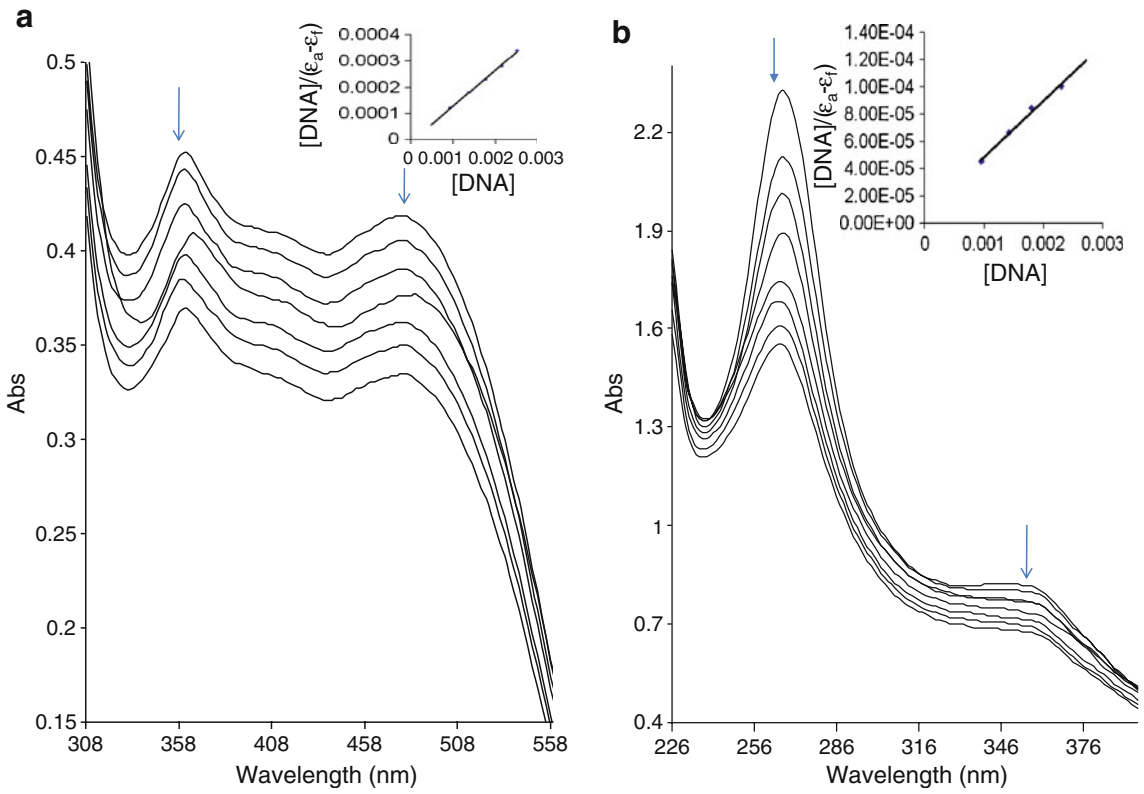


**Fig. 4** Absorption spectra of complexes (**a**) $[Ru(en)_2dppz\text{-}CH_3]^{2+}$ (**b**) $[Ru(en)_2dppz\text{-}NO_2]^{2+}$, tris buffer upon addition of CT DNA in absence (top) and presence of CT DNA (lower) the [Ru]=15 μm; [DNA]=0–126 μm, Insert: plots of $[DNA]/(\Sigma_a-\Sigma_f)$ vs [DNA] for the titration of DNA with complex . Solid line is linear fitting of the data. Arrow shows change in absorption with increasing DNA concentration

Among dppz and dppn ligand the dppn is more plannar. Hence $[Ru(bpy)_2(dppn)]$ form more stable complexes than with dppz. Among the dppz-$NO_2$ and dppz-$CH_3$ complexes dppz-$NO_2$ complex bind strongly to DNA. $NO_2$ is electron withdrawing and $CH_3$ is electron donor. Hence $NO_2$ makes the dppz more electron deficient, which interacts strongly with polyanion DNA than dppz-$CH_3$ [34].

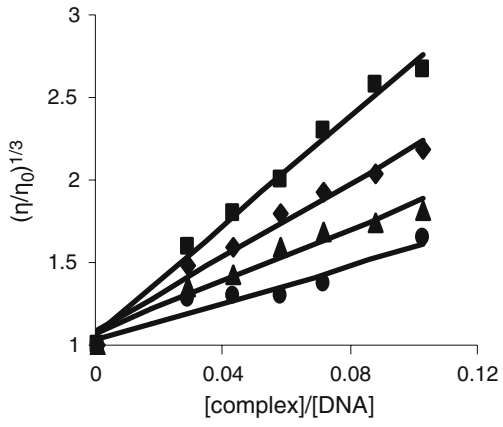


**Fig. 5** Effect of increasing amounts of ethidium bromide (*Black square*), complex 3 (*Black diamond suit*), complex 2 (*Black up-pointing triangle*) and complex 1 (*Black circle*) on the relative viscosity of calf thymus DNA at 25(±0.1)$^0$C. [DNA]=1 mM [Ru]= 5 μM

## Viscosity Measurements

A classical intercalation model demands that the DNA helix must lengthen as base pairs are separated to accommodate the binding ligand, leading to the increase of DNA viscosity. In contrast, a partial intercalation of ligand could bend the DNA helix, reduce its effective length and, concomitantly, its viscosity [31, 43]. The effect of complexes (1), (2) and (3) on the viscosity of rod-like DNA are shown in Fig. 5. For complex (3) & (2) upon increasing the amount of complex, the viscosity of DNA increases

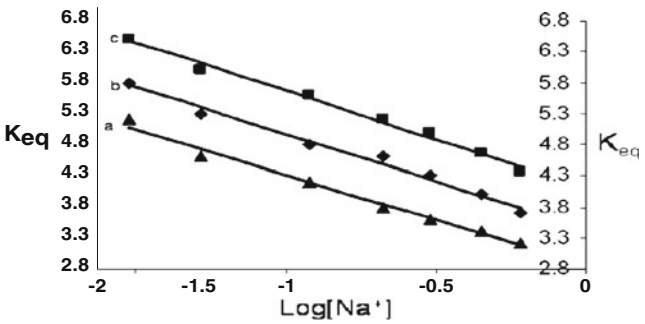


**Fig. 6** Salt dependence of the equilibrium binding constants for DNA binding of complexes **a** $[Ru(en)_2dppz\text{-}CH_3]^{2+}$ **b** $[Ru(en)_2dppz\text{-}No_2]^{2+}$and **c** $[Ru(en)_2dppn]^{2+}$. The lines indicates the slope of the linear square fit to the data as (**a**)-1.26 (**b**)-1.53 (**c**)-1.60

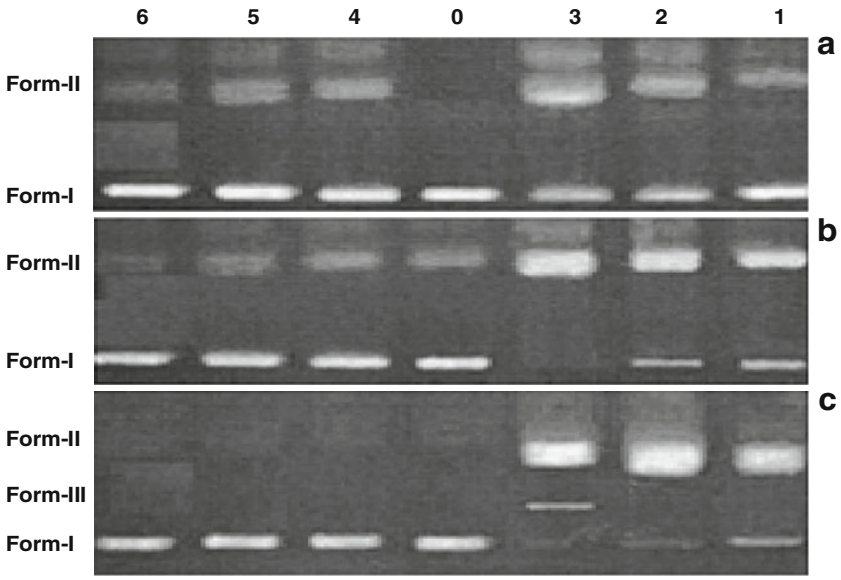


**Fig. 7** Photo cleavage of pBR 322 DNA, in absence and in the presence of complexes **a** $[Ru(en)_2dppn]^{2+}$ **b** $[Ru(en)_2dppz\text{-}No_2]^{2+}$ and **c** $[Ru(en)_2dppn]^{2+}$ after 60 min irradiation at 302 nm. Lane 0 is control plasmid DNA (untreated pBR 322), lane1–3 5 μM, 15 μM, 30 μM addition of complex to pBR 322 DNA. Lane 4–6 5 μM, 15 μM, 30 μM addition of complex in the presence of Histidine (10 mM of Histidine is used in each lane)

steadily, while for the complexes (1) the increase is less. The increase in viscosity for complexes 1,2 & 3 is less when compared to ethidium bromide. The increased degree of viscosity, which may depend on the intercalative affinity for DNA, and follows the order 1<2<3<EB.

## Thermal Denaturation Studies

The melting temperature is defined as the temperature where half of the total base pairs are unbound. According to the literature [44–46] the intercalation of natural or synthesized organics and metallointercalators generally results in a considerable increase in melting temperature ($T_m$). As intercalation of the complexes into DNA base pairs causes stabilization of base stacking and hence raises the melting temperature of the double-stranded DNA. Here $T_m$ of CT-DNA was found to be 60.8 °C in tris-buffer, with addition of the complex (20 μl) to DNA, $T_m$ increases to 64 °C, 66 °C and 67 °C respectively for complex 1,2 & 3. These results also show the interaction of complex 3 with DNA is the strongest among the three complexes.

## Salt Dependence Studies

Figure 6 shows the salt dependence of complex 1, 2 and 3 to DNA. As the concentration of salt (NaCl) increases the binding constant decreases. The dependence of binding constant for these complexes upon $Na^+$ concentration is a consequence of the linkage of complex and $Na^+$ binding to DNA and may be analyzed by polyelectrolyte theory [47].

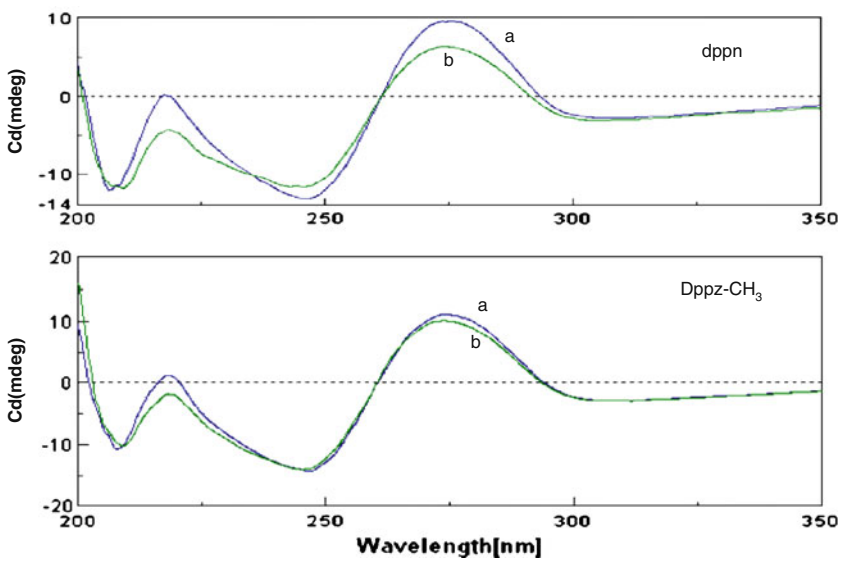


**Fig. 8** Circular dichroism spectra of CT DNA in the absence (**a**) and presence of complex (**b**), after 24 h dialysis.

**Table 3** Circular dichroism spectral data of complexes

| Complexes | Positive peak(nm) | Negative peak(nm) | [θ]in degrees |
|---|---|---|---|
| $[Ru(en)_2dppz\text{-}CH_3]^{2+}$ | 275 | 245 | 16095 |
| $[Ru(en)_2dppz\text{-}No_2]^{2+}$ | 275 | 245 | 17150 |
| $[Ru(en)_2dppn]^{2+}$ | 275 | 246 | 17360 |

From the theory, the slope of the lines in Fig. 6 provides an estimate of Zψ, where ψ is the fraction of counter ions associated with each DNA phosphate(ψ=0.88 for DNA) and Z is the charge on the complex (Z=+2). The slopes of the lines in Fig. 6 are being -1.26, -1.53 and -1.60 for 1, 2 and 3 complexes respectively. These values are less than the theoretically expected values of Zψ (2×0.88=1.76). Such lower values could arise from coupled anion release or from change in complex or DNA hydration upon binding [31]. The knowledge of Zψ allows for a quantitative estimation of the nonelectrostatic contribution to the DNA binding constant for these complexes.

## Photo-Activated Cleavage of pBR322 DNA

After establishing the binding abilities of Ru(II) complexes with DNA, cleavage experiments were performed with pBR322 DNA irradiated for 60 min at 302 nm. The changing of form-I (Supercoiled) through form-II (nicked) and form-III (linear) was observed with increase in concentration of the complexes. Figure 7 Lane 0 is the control pBR322 DNA which do not show any cleavage. It was noted earlier that a single cut on a strand of super coiled DNA relaxes the super coiling and leads to form-II. A second cut of the complementary strand linearizes the DNA and gives form-III. [48–50]. The form-III is observed for $[Ru(en)_2dppn]$ complex at 30 μM of complex concentraction. It is of interest to note that these complexes have been reported to involve a singlet-oxygen ($^1O_2$) mediated DNA photocleavage mechanism [51]. To identify the nature of the reactive species responsible for this mechanism, we have studied with potentially $^1O_2$ inhibiting agent histidine. In the presence of histidine (10 mM) the cleavage is absent (form-II is not observed) or is very less compared to complex with DNA (absence of histidine) Fig. 7 (lane4–6). This indicates that singlet-oxygen plays an important role in the photocleavage mechanism.

## Circular Dichroism Spectral Studies

CD spectrum of Calf thymus DNA consists of a positive band at 275 nm due to base stacking and a negative band at 246 nm due to helicity and is characteristic of DNA in the right- handed B form [52]. The changes in CD signals of DNA observed on interaction with complex may often be assigned to corresponding changes in DNA structure [53]. Thus simple groove binding and electrostatic interaction of small molecules shows less (or) no perturbation on the base stacking and helicity, while intercalation enhances the intensities of both the bands stabilizing the right–handed B conformation of CT DNA [54]. In the presence of the complex, interestingly without the shift in the band positions Molecular ellipticity values, of both positive and negative peaks increases. Complex 3 show a large decrease in intensity, compared with complex 1 and 2 given in Fig. 8. This reveals the effect of strong intercalation of the complexes on base stacking and decreased right-handedness of CT-DNA as well [52]. The Molecular ellipticity values are given in (Table 3) and follows the order as 1<2<3.

## Anti-Microbial Activity

Complexes 1, 2, &3 were dissolved in 2 ml of DMSO and it was added to presterilized Watson's complete basal media [55] at different concentrations viz. 0.1 ml/20 ml, 0.2 ml/20 ml, 0.4 ml/20 ml & 0.8 ml/20 ml of Watson's complete

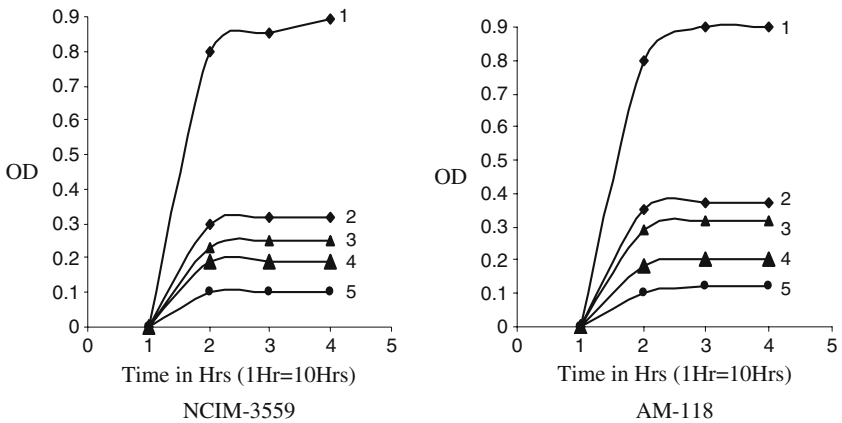


**Fig. 9** Effect of complex $[Ru(en)_2dppz\text{-}NO_2]^{2+}$ on *Saccharomyces cereviseae-NCIM 3559* and *Saccharomyces cereviseae - AM-118* growth expressed on the bases of OD versus time (1 h=10 h)( series 1=control, series 2–5 are 0.1 ml, 0.2 ml, 0.3 ml, 0.4 ml (10 mg in 20 ml)

basal medium. These yeast cultures (Saccharomyces cerevisiae AM 118 & Saccharomyces cerevisiae NCIM 3558) are incubated at 30 °C in a BOD incubator with a cell concentration of 0.1 ml along with control and growth was recorded at equal time intervals from 18 to 51 h for each concentration. The Antimicrobial activities increased as the concentraction of complex increased. It is known that in a complex the positive charge of the metal is partially shared with the donor atoms present in the ligand and there may be electron delocalization over the whole chelate ring. This increases the lipophilic character of the complex and favours its permeation through the lipid layer of bacterial membranes. The results shown in Fig. 9 indicate that all complexes are growth inhibitory and toxic in the order 1<2<3.

## Conclusions

Ruthenium(II) complexes have been synthesized and characterized. Results of absorption, fluorescence, quenching, thermal denaturation, viscosity, circular dichroism, gel electrophoresis and anti microbial activity suggests that complex 2, 3 binds to DNA via an intercalative mode. Complex 1 binds to DNA through an electrostatic mode, which shows that the binding constant and Molecular ellipticity is less. DNA-complex binding is believed to be the key reaction responsible for the anticancer activity of the compounds.

**Acknowledgments** We are grateful to the UGC (New Delhi) for financial support in the form of Major Research Project, and also thankful to Dr. Bhanuprakash (Scientist, NIN) for providing CD facilities.

## References

1. Williams AF, Piguet C, Bernardinelli G (1991) A self-assembling triple-helical $Co_2^{II}$ complex: synthesis and structure. Angew Chem Int Edit 30:1490–1492
2. Hurley DJ, Tor Y (2002) Ru(II) and Os(II) nucleosides and oligonucleotides: synthesis and properties. J Am Chem Soc 124:3749–3762
3. Felder D, Nierengarten JF, Barigelletti F, Ventura BN, Armaroli N (2001) Highly luminescent Cu(I)− phenanthroline complexes in rigid matrix and temperature dependence of the photophysical properties. J Am Chem Soc 123:6291–6299
4. Baek N, Kim H, Hwang G, Kim B (2001) Synthesis and luminescent properties of novel silicon-based electroluminescent copolymers with ruthenium(II)-chelated complexes. Mol Cryst Liq Cryst 370:387–390
5. Connors PJ, Tzalis JD, Dunnic AL, Tor Y (1998) Coordination compounds as building blocks: single-step synthesis of heteronuclear multimetallic complexes containing $Ru^{I}$ and $Os^{II}$. Inorg Chem 37:1121–1123
6. Liu QD, Jia WL, Wang SN (2005) Blue luminescent 2-(2‘-Pyridyl)benzimidazole derivative ligands and their orange luminescent mononuclear and polynuclear organoplatinum(II) complexes. Inorg Chem 44:1332–1343
7. Barton JK, Dannenberg JJ, Raphael AL (1982) Enantiomeric selectivity in binding tris(phenanthroline)zinc(II) to DNA. J Am Chem Soc 104:4967–4969
8. Barton JK, Raphael AL (1984) Photoactivated stereo specific cleavage of double helical DNA by cobalt(III) complexes. J Am Chem Soc 106:2466–2468
9. Barton JK, Danishefsky AT, Goldberg JM (1984) Tris(phenanthroline)ruthenium(II): stereoselectivity in binding to DNA. J Am Chem Soc 106:2172–2176
10. Barton JK, Raphael AL (1985) Site-specific cleavage of left-handed DNA in pBR322 by L-$Co(DIP)_3^{3+}$. Proc Natl Acad Sci USA 82:6460–6464
11. Kumar CV, Barton JK, Turro NJ (1898) Photophysics of ruthenium complexes bound to double helical DNA. J Am Chem Soc 107:5518–5523
12. Nagababu P, Latha JNL, Satyanarayana S (2006) DNA binding studies of mixed-ligand (ethylenediamine)ruthenium(II) complexes. Chem Biodiver 3:1219–1229
13. Nagababu P, Shilpa M, Mustafa MDB, Ramjee P, Satyanarayana S (2008) DNA-binding and photocleavage studies of ethylenediamine cobalt(III) and Ruthenium(II) mixed ligand complexes. Inorg React Mech 6:301–311
14. Erkkila KE, Odom DT, Barton JK (1999) Recognition and reaction of metallointercalators with DNA. Chem Rev 99:2777–2796
15. Pyle AM, Barton JK, Lippard SJ (1990) Progress in inorganic chemistry bio inorganic chemistry. (ed), John Wiley & Sons: New York. 38: 413-475
16. Chow CS, Barton JK (1992) Transition metal complexes as probes of nucleic acids. Meth Enzymol 212:219–242
17. Murphy CJ, Barton JK (1993) Ruthenium complexes as luminescent reporters of DNA. Meth Enzymol 226:576–594
18. Kane-Maguire, NAP, Wheeler JF (2001) Photo redox behavior and chiral discrimination of DNA bound $M(diimine)_3^{n+}$ complexes ($M=Ru^{2+}$, $Cr^{3+}$). Coord Chem Rev 211:145-4-162
19. Norden B, Lincoln P, Akerman B, Tuite E (1996) Metal Ions in Biological Systems. In Sigel A, Sigel H (eds) Marcel Dekker, New York 33:177-252
20. Kelly SO, Barton JK (1999) Metal ions in biological systems. In Sigel A, Sigel H (eds) Marcel Dekker, New York 39:211-249
21. Pyle AM, Rehmann JP, Meshoyrer R, Kumar CV, Turro NJ, Barton JK (1989) Mixed-ligand complexes of ruthenium(II): factors governing binding to DNA. J Am Chem Soc 111:3051–3058
22. Yamada M, Tanaka Y, Yoshimoto Y, Kuroda Shimao S (1992) Synthesis and properties of diamino-substituted Dipyrido[3, 2-a:20, 30-c]Phenazine. J Bull Chem Soc Jpn 65:1006–1011
23. Marmur J (1961) A procedure for the isolation of DNA from microorganisms. J Mol Biol 3:208–218
24. Reichmann ME, Rice SA, Thomas CA, Doty P (1954) A further examination of the molecular weight and size of desoxypentose nucleic acid. J Am Chem Soc 76:3047–3053
25. Dickeson JE, Summers LA (1970) Derivatives of 1, 10-Phenanthroline-5, 6-quinone Aus. J Chem 23:1023–1027
26. Sullivan BP, Salmon DJ, Meyer T (1978) Mixed phosphine 2, 2′-bipyridine complexes of ruthenium. Inorg Chem 17:3334–3341
27. McGhee JD, Von Hippel PH (1974) Theoretical aspects of DNA-protein interactions: co-operative and non-co-operative binding of large ligands to a one-dimensional homogeneous lattice. J Mol Biol 86:469–489
28. Lakowicz JR, Webber G (1973) Quenching of fluorescence by oxygen. Probe for structural fluctuations in macromolecules. Biochemistry 12:4161–4170
29. Wolfe A, Shimer GH Jr, Meehan T (1987) Polycyclic aromatic hydrocarbons physically intercalate into duplex regions of denatured DNA. Biochemistry 26:6392–6396

30. Chaires JB, Dattagupta N, Crothers DM (1982) Self association of daunomycin. Biochemistry 21:3927–3932
31. Satyanarayana S, Dabrowiak JC, Chaires JB (1993) Tris (phenanthroline) ruthenium(II) enantiomer interactions with DNA: mode and specificity of binding. Biochemistry 32:2573–2584
32. Tselepi-Kalouli E, Katsaros N (1989) The interaction of [Ru $(NH_3)_5CI]^{2+}$ and $[Ru(NH_3)_6]^{3+}$ ions with DNA. J Inorg Biochem 37:271–282
33. Kumar CV, Barton JK, Turro NJ (1985) Photophysics of ruthenium complexes bound to double helical DNA. J Am Chem Soc 107:5518–5523
34. Liu J, Mei WJ, Lin Li J, Zheng KC, Chao H, Yun FC, Ji LN (2004) Electronic effects on the interactions of complexes [Ru $(phen)_2(p\text{-}L)]^{2+}$ (L= MOPIP, HPIP, and NPIP) with DNA. Inorg Chem Acta 357:285–293
35. Wu J, Du F, Zhang P, Khan IA, Chen J, Liang Y (2005) Thermodynamics of the interaction of aluminum ions with DNA: Implications for the biological function of aluminum. J Inorg Biochem 99:1145–1154
36. Lakowicz JR (1983) Principles of fluorescence spectroscopy. Plenum Press, New York
37. Barton JK, Lolis E (1985) Chiral discrimination in the covalent binding of bis(phenanthroline)dichlororuthenium(II) to B-DNA. J Am Chem Soc 107:708–709
38. Rajesh B, Nair L, Yeung K, Murphy C (1999) Synthesis and solvent-dependent properties of Ru(acac)2d ppz. J Inorg Chem 38:2536–2538
39. Chen L-M, Liu J, Chen J-C, Tan C-P, Shi S, Zheng K-C, Ji L-N (2008) Synthesis, characterization, DNA-binding and spectral properties of complexes $[Ru(L)_4(dppz)]^{2+}$ (L = Im and MeIm). J Inorg Biochem 102:330–341
40. Pyle AM, Rehmann JP, Meshoyrer MR, Kumar CV, Turro NJ, Barton JK (1989) Mixed-ligand complexes of ruthenium(II): factors governing binding to DNA. J Am Chem Soc 111:3051–3058
41. Ji L, Zhang Q, Liu J (2001) DNA structure, binding mechanism and biology functions of ppolyp[yridyl complexes in biomedicine. Sci China series B 44:246–259
42. Laxma Reddy K, Harish Kumar Reddy Y, Satyanarayana S (2009) DNA-binding and photocleavage properties of Ru(II) Polypyridyl complexes with DNA and their toxicity studies on eukaryotic microorganisms. Nucleosides Nucleotides Nucleic Acids 28:953–968
43. Satyanarayana S, Dabrowiak JC, Chaires JB (1992) Neither Δ- nor Λ- tris(phenanthroline(ruthenium)(II) binds to DNA by classical intercalation. Biochemistry 31:9319–9324
44. Waring MJ (1965) Complex formation between ethidium bromide and nucleic acids. J Mol Biol 1965(13):269–282
45. Neyhart GA, Grover N, Smith SR, Kalsbeck WA, Fairly TA, Cory M, Thorp HH (1993) Binding and kinetics studies of oxidation of DNA by oxoruthenium(IV). J Am Chem Soc 115:4423–4428
46. Kelly JM, Tossi AB, McConnell DJ, OhUigin C (1985) A study of the interactions of some polypyridylruthenium (II) complexes with DNA using fluorescence spectroscopy, topoisomerisation and thermal denaturation. Nucleic Acids Res 13:6017–6034
47. Record MT Jr, Anderson CF, Lohman TM (1978) Thermodynamic analysis of ion effects on the binding and conformational equilibria of proteins and nucleic acids: the roles of ion association or release, screening, and ion effects on water activity. Q Rev Biophys 11:103–178
48. Basile LA, Barton JK (1987) Design of a double-stranded DNA cleaving agent with two polyamine metal-binding arms: Ru $(DIP)_2$Macron. J Am Chem Soc 109:7548–7550
49. Gorver N, Guptha N, Singh P, Thorp H (1992) Studies of electrocatalytic DNA cleavage by oxoruthenium(IV). X-ray crystal structure of [Ru(tpy)(tmen)OH2](ClO4)2 (tmen = N, N, N', N'-tetramethylethylenediamine, tpy = 2, 2′, 2″-terpyridine). Inorg Chem 31:2014–2020
50. Kishikawa H, Jiang YP, Goodisman J, Dabrowiak JC (1991) Coupled kinetic analysis of cleavage of DNA by esperamicin and calicheamicin. J Am Chem Soc 113:5434–5440
51. Mei HY, Barton JK (1988) Tris(tetramethylphenanthroline)Ruthenium(II): a chiral probes that cleaves A-DNA conformations. Proc Natl Acad Sci USA 85:1339–1343
52. Ivanov VI, Minchenkova LE, Schyolkina AK, Poletayer AI (1973) Different conformations of double-stranded nucleic acid in solution as revealed by circular dichroism. Biopolymers 12:89–110
53. Lincoln P, Tuite E, Norden B (1997) Short-Circuiting the Molecular Wire: Cooperative Binding of Δ-[Ru(phen)2d ppz]2+ and Δ-[Rh(phi)2bipy]3+ to DNA. J Am Chem Soc 119:1454–1455
54. Norden B, Tjerneld F (1982) Structure of methylene blue–DNA complexes studied by linear and circular dichroism spectroscopy. Biopolymers 21:1713–1734
55. Nagababu P, Shilpa M, Satyanarayana S, JNl L, Karthikeyan KS, Rajesh M (2008) Interaction of cobalt(III) polypyridyl complexes containing asymmeteric ligands with DNA. Transit Met Chem 33:1027–1033